ESC European Society of Cardiology

Europace (2022) **24**, 747–754
https://doi.org/10.1093/europace/euab271

Clinical utility of non-contact charge density 'SuperMap' algorithm for the mapping and ablation of organized atrial arrhythmias

Michael T.B. Pope [1,2]*, Milena Leo[1], Andre Briosa e Gala[1,2], and Timothy R. Betts [1,3]

[1]Department of Cardiology, Oxford University Hospitals NHS Foundation Trust, Oxford, UK; [2]Department for Human Development and Health, University of Southampton, Southampton, UK; and [3]Division of Cardiovascular Medicine, University of Oxford Biomedical Research Centre, Oxford, UK

Received 23 July 2021; editorial decision 7 October 2021; accepted after revision 11 October 2021; online publish-ahead-of-print 6 December 2021

Aims SuperMap is a novel non-contact algorithm for the mapping of organized atrial arrhythmias. We prospectively evaluated SuperMap during mapping and ablation of atrial tachycardias (ATs) and paced rhythms and compared to conventional high-density contact mapping.

Methods and results Consecutive patients undergoing SuperMap guided ablation of pre-existing ATs or AT developed during atrial fibrillation ablation procedures were included together with maps obtained during pacing to assess block in linear lesions. The time taken to obtain diagnostic maps was measured together with the number of electrogram (EGM) points and accuracy compared to the arrhythmia diagnosis confirmed using a combination of map findings, entrainment, and response to ablation. In a subgroup of patients, concurrent contact mapping was performed with contact and SuperMap analysed by separate operators blinded to the other technique. The time taken to generate a diagnostic map, EGM number, and map accuracy was compared. Thirty-one patients (62 maps) were included with contact mapping performed in 19 [39 maps (33 for AT)]. SuperMap acquisition time was 314 s [interquartile range (IQR) 239–436]. The median number of EGM points used per map was 5399 (IQR 3279–8677). SuperMap was faster than contact mapping [394 ± 219 s vs. 611 ± 331 s; difference 217 s, 95% confidence interval (CI) 116–318, $P < 0.0005$]. The number of EGM points used per map was higher for SuperMap (7351 ± 5054 vs. 3620 ± 3211; difference 3731, 95% CI 2073–5388, $P < 0.0005$). SuperMap and contact mapping were accurate in 92% and 85% of maps, respectively, $P = 0.4805$.

Conclusion SuperMap non-contact charge density mapping is a rapid and reliable approach to guide the ablation of complex atrial arrhythmias.

Keywords Non-contact mapping • Atrial tachycardia • Ablation • SuperMap algorithm

Introduction

Atrial arrhythmias may arise either *de novo* or as a result of substrate development following catheter ablation or cardiac surgery. Mechanisms can be highly complex including focal (encompassing both automaticity or micro-reentry) and macro-reentry circuits. Electroanatomical mapping can be challenging when using traditional sequential contact techniques, particularly when the cycle length varies and rhythms are non-sustained.[1–3]

Non-contact charge density mapping (Acutus Medical) has been used for the mapping and ablation of atrial fibrillation (AF) with promising early results.[4] More recently, a novel algorithm for high-resolution non-contact mapping of organized atrial rhythms has been developed, termed 'SuperMap'. Early work has demonstrated the

* Corresponding author. Tel: 0286520255. *E-mail address*: michael.pope@ouh.nhs.uk

What's new?

- The multi-position 'SuperMap' charge density algorithm is a novel, non-contact approach to guide mapping and ablation of complex atrial tachycardias.
- Mapping accuracy is equivalent to contemporary high-density contact mapping.
- 'SuperMap' allows faster generation of diagnostic activation maps compared to contact mapping with a higher density of electrogram points.

feasibility of this system in a small cohort of patients undergoing ablation of complex atrial tachycardias (ATs) after AF ablation but there has been no systematic evaluation of its accuracy and clinical utility.[5] We sought to prospectively evaluate the application of this novel non-contact approach in a series of patients during mapping and ablation of ATs and to confirm bidirectional block across linear ablation lesions during pacing in comparison to conventional high-density contact mapping.

Methods

Patient selection

Consecutive patients undergoing SuperMap non-contact mapping of organized ATs and during pacing for assessment of block in subsequent linear ablation lesions were prospectively studied following written informed consent. Patients either presented for ablation of pre-existing AT or developed AT during an AF ablation procedure. Patients were enrolled in parallel research studies including DISCOVER (clinicaltrials.gov NCT04431544) or CASDAF-HD (clinicaltrials.gov NCT04229472). The study complied with the principles of the Declaration of Helsinki.

Electrophysiological mapping and ablation

Procedures were carried out under general anaesthetic. Except for amiodarone, antiarrhythmic drugs were stopped a minimum of 5 days prior to the procedure when possible. Venous access was obtained through bilateral femoral vein puncture under direct ultrasound guidance. A decapolar catheter (Inquiry, Abbott Medical) was inserted into the coronary sinus (CS) and an AcQRef (Acutus Medical) sheath or quadripolar catheter (with distal electrode passed just beyond the access sheath) was used to provide an indifferent electrode as a unipolar reference. In patients where left atrial (LA) access was required, heparin boluses were administered prior to trans-septal puncture followed by continuous infusion to maintain an activated clotting time >350 s. A single trans-septal puncture was used with an ablation catheter advanced alongside via an Agilis steerable sheath.

The AcQMap (Acutus Medical) catheter was advanced into the chamber of interest over a 0.032 guidewire via an AcQGuide (Acutus Medical) sheath. In patients attending for ablation of known AT, mapping was performed at this stage with arrhythmias induced using burst pacing from the CS when necessary. In patients undergoing AF ablation procedures, ablation was performed using the AcQMap system as previously described.[6,7] Where AT arose following targeted ablation, mapping was undertaken and included in the analysis.

In a subgroup of patients, concurrent mapping was performed using the Ensite Precision (Abbott Medical) electroanatomic mapping system. Electroanatomic mapping data were collected using either an HD-grid or Advisor Variable Loop circular mapping catheter (Abbott Medical). Ablation was delivered using an irrigated force-sensing ablation catheter [Tacticath or AcQBlate (Biotronik)]. Arrhythmia mechanisms were confirmed according to a combination of electroanatomic mapping findings, response to entrainment, and response to ablation.

Non-contact mapping procedure

Non-contact mapping was performed using the AcQMap catheter (Acutus Medical), a spheroid shaped catheter consisting of six splines with eight electrodes and eight ultrasound transducers on each spline. The endocardial surface was approximated by reflected points from ultrasound while roving the catheter inside the heart chamber. The 48 non-contact electrodes measure the intracardiac electrical field and distributed charge densities were computed on the endocardial surface by solving the inverse problem. A 'SuperMap' algorithm allows accumulating of the non-contact measurements by aligning different beats acquired at different times and at different locations of the chamber during repetitive rhythms, e.g. ATs, sinus and paced rhythms. The atrial surface in proximity to the roving electrodes is highlighted during data collection to guide adequate spatial distribution of measurements (*Figure 1*). Unipolar electrograms (EGMs) simultaneously recorded in the CS were used as a timing reference to align the beats and those beats were grouped with similar morphologies. Charge densities were then computed by grouped beats, and the propagation history, an animated leading wavefront with colour-coded activation histories, was generated for visualization. Further detail on the SuperMap non-contact algorithm is contained within the Supplementary material online.

Data collection and analysis

The primary outcome was the total time taken to obtain a non-contact map. Time zero was recorded as the point of insertion of the catheter into the chamber of interest and measured until map analysis was complete and an ablation strategy could be devised based on the propagation map generated. Where the chamber anatomy was already generated (for example in the case of AT arising following AcQMap-guided ablation of AF) then the time for anatomy generation was not included but in all other cases, this was included in the total time. The components of the total mapping time including multi-position recording time and map processing/analysis were also measured.

In a subgroup of patients in whom concurrent contact mapping was conducted, SuperMap non-contact mapping was performed initially as mapping data is not visualised during collection, so the primary operator is blinded to the mapping results. The contact map was then performed with the primary operator able to visualize collection of points in the normal fashion. A second experienced operator analysing the SuperMap non-contact map was blinded from viewing the contact map resulting in separate collection of timing and mapping diagnosis by operators blinded to the findings of the other technique. The diagnosis and ablation strategy determined by each map was recorded separately allowing comparison of concordance and relative accuracy of each method. The total time for generation of contact maps was measured from the point of insertion of the mapping catheter to the time that map interpretation was complete to allow comparison between the two methods. The number of EGM signals used to generate each map was also compared. Final accuracy of each map was determined against the confirmed arrhythmia diagnosis obtained from a combination of electroanatomic mapping findings, response to entrainment (when possible) and the response to ablation.

Figures were generated and statistical analysis conducted using Matlab (Mathworks, R2019a). Data are expressed as mean ± standard deviation or median and interquartile range (IQR) depending on distribution.

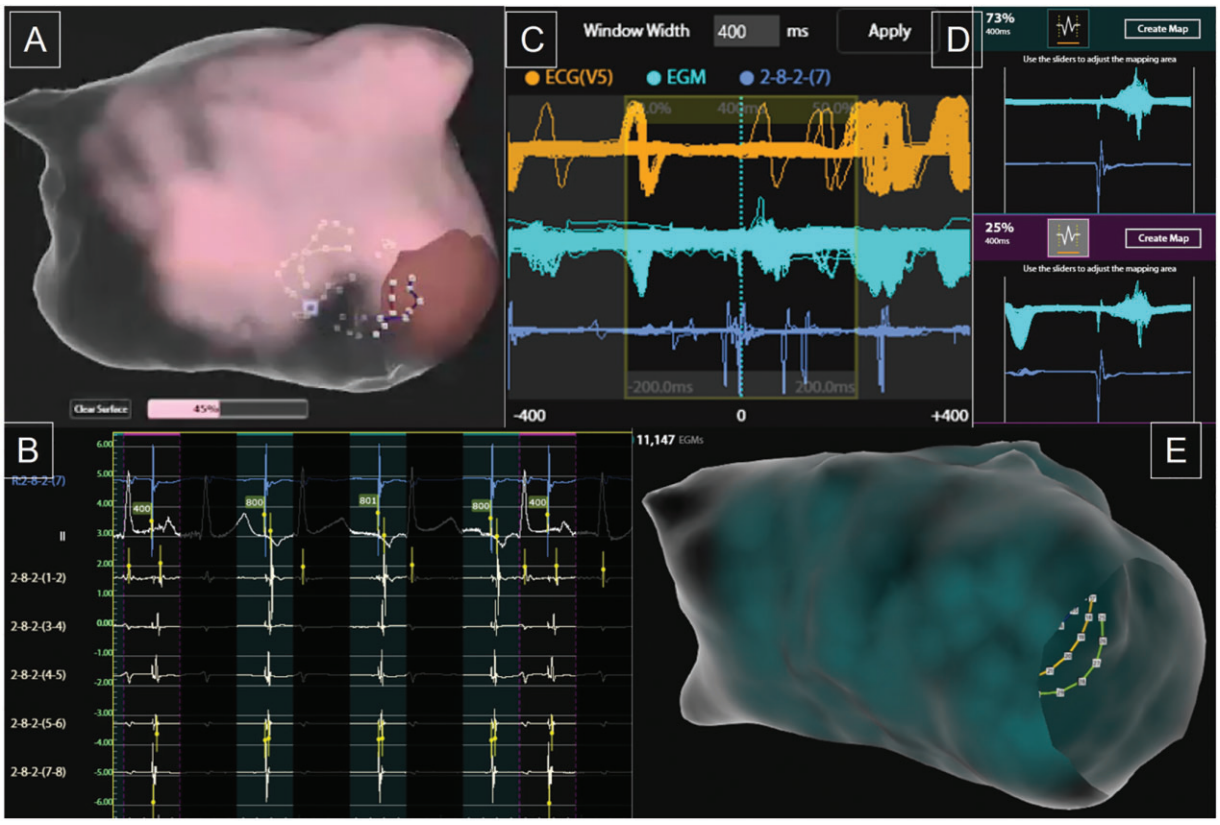

Figure 1 Example of SuperMap acquisition during pacing using a repeating 3-beat drive train at 800 ms cycle length followed by a single extrastimulus at 400 ms cycle length. SuperMap non-contact multi-position atrial electrogram data are obtained during continuous manipulation of the AcQMap catheter throughout the chamber with the surface illuminating once adequate proximity has been obtained (*A*). The proportion of the surface covered is updated throughout. Each cycle detected is grouped according to coronary sinus electrogram cycle length and morphology, with 800 ms paced beats highlighted in green and extrastimulus beats in pink (*B*). The window of interest can be adjusted as required (*C*) and the proportion of data within each beat group identified (*D*). The group of interest can be selected to show the density and number of non-contact electrograms included (*E*) and generate a propagation history map of wavefront activation.

Mapping times and number of EGM points were compared using the paired *t*-test, whilst the proportion of maps deemed accurate was compared using the Fisher's exact test. A two-sided *P*-value of <0.05 was considered significant.

Results

Patients included

A total of 31 patients were included in whom SuperMap non-contact mapping was used for assessment of either AT or during pacing to assess block in linear ablation lesions, with a total of 62 maps obtained. Baseline characteristics for all patients are included in *Table 1*. The median age of patients was 64 (IQR 59–70), and 58% were male. Twenty-three patients had undergone previous ablation and 5 had undergone cardiac surgery. Parallel high-density contact mapping was performed in 19 patients (resulting in 39 maps) for comparison. In both groups, AT was the predominant rhythm analysed as illustrated in *Table 2*.

SuperMap non-contact acquisition and mapping characteristics

The median time for anatomy generation was 152 s (IQR 122–192) and mapping data were simultaneously collected during the anatomy build on three occasions. The median time for collection of multi-position non-contact data was 165 s (IQR 125–210) with processing and analysis requiring a further 104 s (IQR 77–174) and a total time to reach a map diagnosis of 314 s (IQR 239–436). The median number of EGM points per map used was 5399 (IQR 3279–8677).

Table 3 shows the arrhythmia mechanisms of all ATs identified. The mean cycle length was 301 ± 92 ms. Focal tachycardias were the most common mechanism identified ($n = 17$), followed by mitral isthmus dependent macro-reentry ($n = 9$). Across all maps analysed, SuperMap non-contact mapping was accurate in 95%, and 96% when only ATs were included. Non-contact mapping was considered inaccurate in three maps:

(1) Highly scarred atrium resulted in highly fractionated and low amplitude CS EGMs which caused inaccurate beat grouping and an

Table 1 Patient baseline characteristics

Patient characteristics	*n* (%)
Total patients	31
Male	18 (58)
Age	64 (IQR 59–70)
AA drug during the procedure	6 (19)
Flecainide	2 (6.4)
Amiodarone	2 (6.4)
Sotalol	1 (3.2)
Propafenone	1 (3.2)
SR at start	11 (35)
AF at start	10 (32)
AT at start	10 (32)
Prior ablation	23 (74)
Prior PVI	22 (71)
Prior CTI	10 (32)
Prior MI	4 (13)
Prior Roof line	7 (23)
Prior PWI	2 (6)
Prior cardiac surgery	5 (16)

Data are expressed as *n* (%) or interquartile range (IQR).
AA, antiarrhythmic drug; AF, atrial fibrillation; AT, atrial tachycardia; CTI, cavo-tricuspid isthmus; MI, mitral isthmus; PVI, pulmonary vein isolation; PWI, posterior wall isolation; SR, sinus rhythm.

Table 2 Breakdown of maps obtained for analysis in all patients and where comparison contact mapping was performed

Maps collected	*n* (%)
Total patients	31
Maps obtained	62
LA	46 (74)
RA	16 (26)
AT	51 (82)
Linear lesions	11 (18)
Number patients with contact maps	19 (61)
Maps obtained	39
AT maps	33 (85)
Linear lesions	6 (15)

AT, atrial tachycardia; LA, left atrium; RA, right atrium.

Table 3 Tachycardia mechanisms identified in all patients

Maps obtained	*N*	Cycle length, ms (mean ± standard deviation)
MI flutter	9	303 ± 62
Roof flutter	6	244 ± 52
CTI flutter	4	336 ± 159
Local re-entry	6	306 ± 61
Focal AT	17	293 ± 96
Line block	8	NA
Line gap	3	NA
Breakthrough[a]	9	336 ± 112

AT, atrial tachycardia; CTI, cavo-tricuspid isthmus; MI, mitral isthmus.
[a]Breakthrough represents mechanisms propagating through from the contralateral chamber to that mapped.

inaccurate map (contact mapping in this case was similarly challenging and did not accurately identify the arrhythmia mechanism).

(2) Human error in processing resulted in incomplete cycle length giving the impression of a focal mechanism in the case of a mitral isthmus dependent flutter.

(3) Artefact during pacing resulted in incorrect interpretation of posterior wall conduction.

Comparison of non-contact and contact mapping

Parallel high-density contact mapping allowed comparison across 19 patients including 33 maps of AT and 6 maps during pacing. In one further patient, contact mapping was attempted but the tachycardia was sustained for only short periods with highly variable cycle length precluding acquisition. SuperMap non-contact mapping correctly identified a focal AT originating from the right upper pulmonary vein.

Contact mapping was conducted using HD-grid in 72% and the Advisor circular mapping catheter in 28% (see Supplementary material online, *Table S1*). The total time for acquisition of SuperMap non-contact maps was 394 ± 219 s compared to 611 ± 331 s for contact mapping, resulting in a significant difference of 217 s [95% confidence interval (CI) 116–318, $P < 0.0005$]. This remained significant when only ATs were included (418 ± 230 vs. 639 ± 335, difference 221 s, 95% CI 106–337, $P < 0.0005$) but there was no significant difference for paced maps (264 ± 56 vs. 455 ± 282, difference 191 s, 95% CI −64 to 447, $P = 0.1125$) (see *Figure 2A*). SuperMap non-contact mapping resulted in a higher number of included EGMs across all maps (7351 ± 5054 vs. 3620 ± 3211, difference 3731, 95% CI 2073–5388, $P < 0.0005$) and in AT maps (7641 ± 5421 vs. 3554 ± 3396, difference 4087, 95% CI 2185–5988, $P < 0.0005$). There was no significant difference in the number of EGMs included for paced maps (5755 ± 1574 vs. 3981 ± 2090, difference 1774, 95% CI −1425 to 4973, $P = 0.2134$) (see *Figure 2B*).

Across all 39 maps compared, SuperMap non-contact, and contact mapping were accurate in 92% and 85% respectively, $P = 0.4805$. In 31 (79%), both mapping methods produced concordant results. In 4 (10%) maps, SuperMap non-contact mapping was accurate and contact maps were inaccurate or uninterpretable whilst in 2 (5%), contact maps were accurate and SuperMap non-contact inaccurate. For maps of AT only, SuperMap non-contact and contact maps were accurate in 94% and 81%, respectively, $P = 0.2597$ (see *Table 4* for full results).

Arrhythmia mechanisms revealed

SuperMap non-contact mapping correctly identified a focal gap in linear ablation lesions during pacing in three maps (one in cavotricuspid isthmus, two in mitral isthmus), which were also seen using contact mapping, allowing delivery of limited focal ablation resulting in

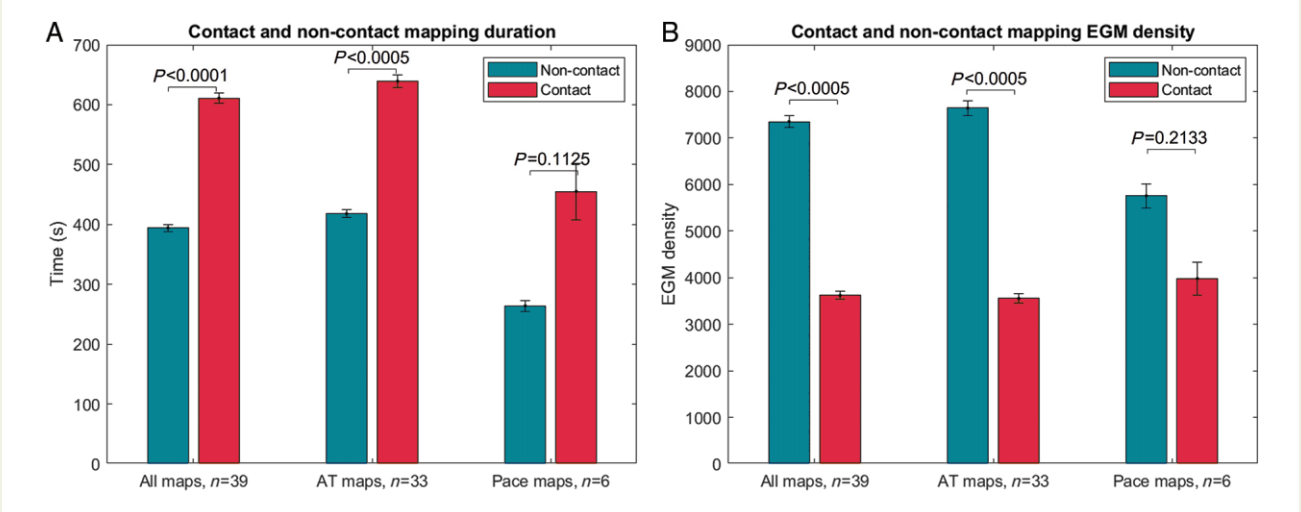

Figure 2 Comparison of map duration and EGM acquisition during SuperMap non-contact and contact mapping. Bars represent standard error of the mean. EGM, electrogram.

Table 4 Comparative accuracy of SuperMap non-contact and contact mapping of all maps and maps of atrial tachycardias only

Map obtained	Map accuracy	*n* (%)
All maps	SuperMap accurate	59 (95)
All AT maps	SuperMap accurate	47 (96)
All timed comparison maps	SuperMap accurate	36 (92)
	Contact accurate	33 (85)
	Both accurate	31 (79)
	SuperMap accurate, contact inaccurate/uninterpretable	4 (10)
	Contact accurate, SuperMap inaccurate	2 (5)
	Both inaccurate	1 (3)
AT timed comparison maps	SuperMap accurate	31 (94)
	Contact accurate	27 (82)
	Both accurate	26 (79)
	SuperMap accurate, contact inaccurate/uninterpretable	4 (12)
	Contact accurate, SuperMap inaccurate	1 (3)
	Both inaccurate	1 (3)
Contact mapping abandoned		1

AT, atrial tachycardia.
In one patient, contact mapping was attempted but abandoned due to non-sustained arrhythmia with highly variable cycle length.

transmural block. In addition, *Figure 3* (Supplementary material online, *Video S1*) shows an example of epicardial conduction across linear LA roof ablation resulting in a roof-dependent flutter. Focal ablation at the site of earliest activation beyond the line resulted in linear block.

Figure 4 shows an example of a focal tachycardia mechanism arising near the base of the LA appendage (LAA) as revealed using SuperMap non-contact mapping. Contact mapping suggested a possible macro-reentry circuit involving the carina between the left pulmonary veins. However, SuperMap non-contact activation mapping shows very delayed activation into the left pulmonary veins (see also Supplementary material online, *Video S2*). Mis-annotation of late EGM signals in the contact map resulted in the appearance of early activation at this site and a misleading map. Entrainment at the posterior wall near the left pulmonary veins revealed a long return time (PPI-TCL 92 ms) whilst entrainment near the base of the appendage on the anterior wall confirmed this area to be within the circuit [post pacing interval (PPI) equal to tachycardia cycle length (TCL), see *Figure 4*] suggesting localised micro-reentry. Ablation at the site of focal origin on non-contact mapping resulted in arrhythmia termination.

Acute procedural outcomes

There were no major procedural adverse events or technical failures of non-contact mapping. In all but one patient ablation resulted in arrhythmia termination and non-inducibility of further atrial arrhythmias. In one patient a focal AT that was easily inducible but non-sustained and with variable cycle length was identified using non-contact mapping with the site of origin near the CS ostium in the right atrium. Ablation at this site resulted in acceleration, but it remained inducible after extensive ablation and the procedure was terminated. The patient suffered further symptomatic narrow complex tachycardias and a repeat procedure was performed after 3 months. At repeat procedure, the arrhythmia was more sustained, and the same mechanism was identified using high-density contact mapping. Ablation at the site of earliest activation resulted in termination and non-inducibility.

Discussion

This study demonstrates the clinical utility of non-contact charge density mapping of organised atrial arrhythmias and pacing.

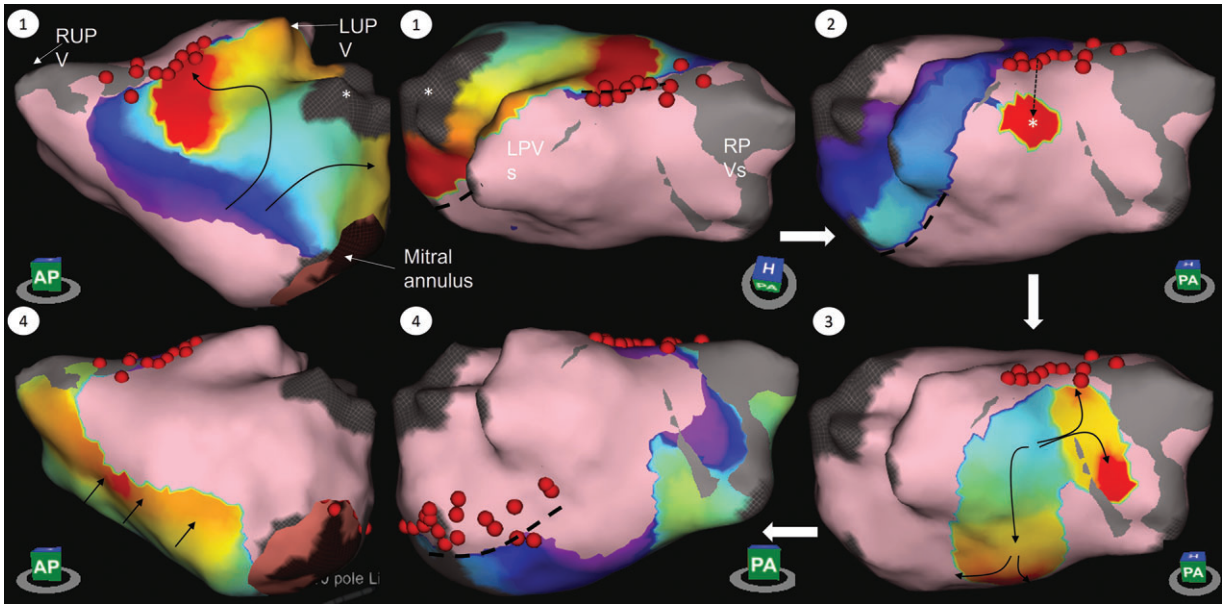

Figure 3 Example of roof-dependent left atrial flutter using an epicardial connection across a roof line with block in the mitral isthmus. The wavefront propagates up the anterior wall appearing to block at the roof (1), followed by the appearance of a focal point of activation on the posterior wall (2) then conducts both superiorly towards the line as well as inferiorly down the back wall (3) with block in the mitral isthmus and activation across the septum towards the anterior LA (4). See also Supplementary material online, *Video S1*. Dotted lines show regions of conduction block; dotted arrow represents course of epicardial conduction; *, left atrial appendage; LPVs, left pulmonary veins; LUPV, left upper pulmonary vein; RPVs, right pulmonary veins; RUPV, right upper pulmonary vein.

SuperMap non-contact mapping was highly accurate, resulting in correct identification of the arrhythmia mechanism or analysis of linear block in 95% of cases. SuperMap non-contact mapping was significantly faster than contact mapping, with a mean difference of 217 s (3 min 37 s) and with a higher EGM density; both differences most evident in mapping of complex AT.

The advent of three-dimensional electroanatomic mapping systems has resulted in excellent rates of acute arrhythmia termination during ablation of ATs even prior to the development of high-density multipolar mapping catheters.[8,9] The use of ultra-high resolution 3D mapping has allowed further characterization of arrhythmia mechanisms, with high acute procedural success rates, albeit with significant recurrent arrhythmias.[10] The bar against which novel methods of electroanatomic mapping are to be compared is therefore extremely high and the accuracy of the SuperMap non-contact algorithm demonstrated in this study compared extremely favourably with that seen using contemporary high-density contact mapping.

Procedural evaluation of ATs often involves a combination of electroanatomic mapping complimented by entrainment manoeuvres to confirm arrhythmia mechanisms.[9,11] However, this confers a risk of termination with the potential for non-inducibility. Similarly, some arrhythmias, particularly focal mechanisms, can be non-sustained, making sequential activation mapping challenging.[12,13] In addition, these techniques can be time consuming. In the study by Winkle *et al.*[14] using high-density contact mapping, the time from initiation of geometry and map creation to the delivery of radiofrequency ablation was 24 ± 11 min, which reduced by 16% to 20 ± 11 min when arrhythmias were induced after geometry creation. In a recent study of mechanisms of recurrent left ATs, the mean mapping time was 1108 ± 515 s (18.4 min), albeit involving collection of extremely high-density contact maps with a mean of 16 229 ± 8222 EGM points.[15] The average time for completion of contact mapping in our study was 611 ± 331 s (10.2 min). This compares highly favourably to the previous studies discussed but was still significantly longer than the time taken using SuperMap non-contact charge density mapping (6.6 min). Rapid collection of accurate high-density activation maps may therefore facilitate the evaluation of mechanisms that are non-sustained with the potential to significantly shorten procedure times.

Importantly, rapid collection of activation maps was not at the expense of either EGM density or accuracy. There were only three maps that were demonstrated to be inaccurate. One of these was not helped by contact mapping and the mechanism (local re-entry through dense anterior wall/septal scar) was only confirmed after multiple non-contact and contact maps as well as entrainment manoeuvres. Human error in processing resulted in erroneous interpretation on one occasion and pacing artefact influenced interpretation in assessment of linear block. In both these scenarios, increasing familiarity and diligence over map creation/calculation would have eliminated these errors.

There is an increasing recognition of the role of the three-dimensional atrial substrate involved in atrial re-entry circuits. Pambrun *et al.*[16] recently described the importance of epicardial connections of the septo-pulmonary bundle facilitating conduction across the LA

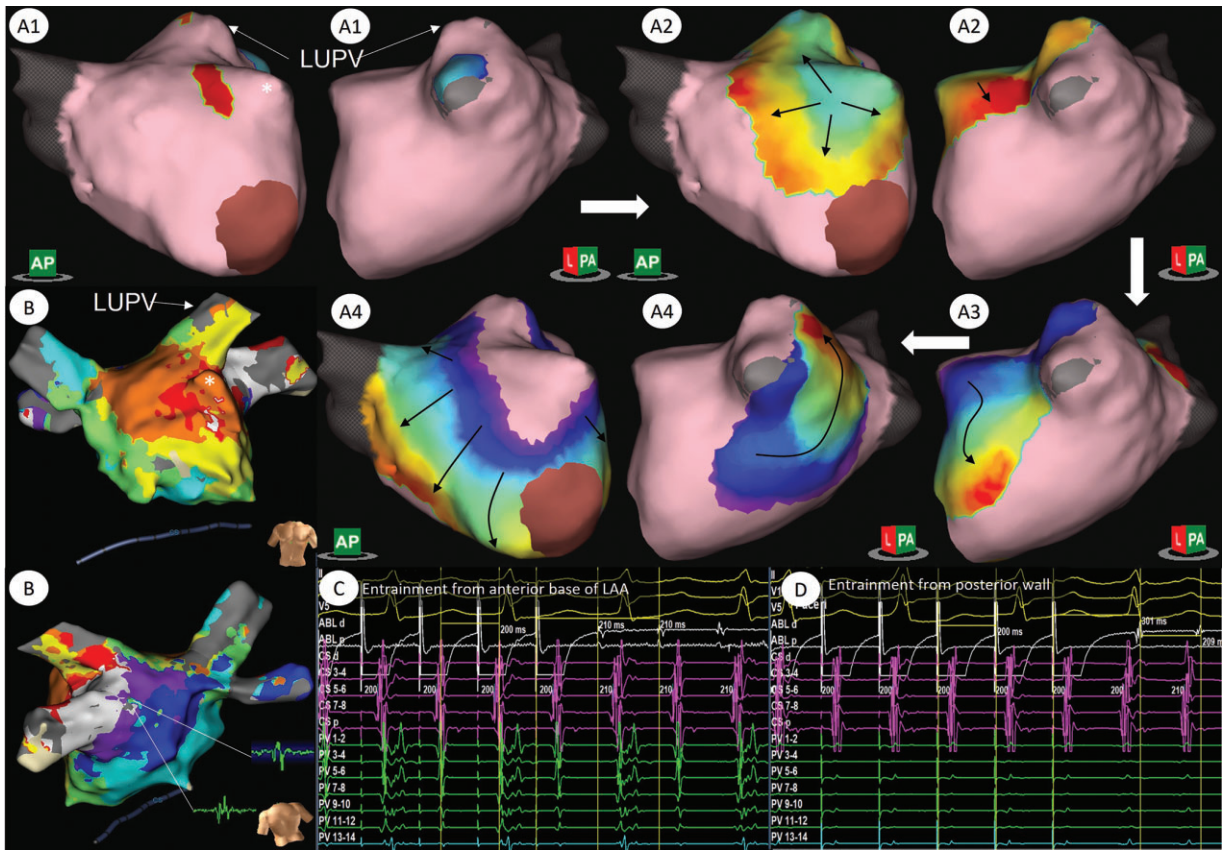

Figure 4 Example of atrial tachycardia mapped using non-contact SuperMap algorithm and HD-grid in a patient with an AT arising following a previous PVI and roof line. *A1–A4* show activation in a centrifugal pattern arising from the anterior base of the LAA with block in the roof and activation through the mitral isthmus with inferior to posterior activation of the posterior wall. In *B*, LAT map generated using the HD grid and Ensite Precision (Abbott Medical) shows a region of 'early-meets-late' activation within the carina between the left pulmonary veins suggestive of a re-entry circuit involving this region and electrograms from this site. Entrainment from the base of the LAA (*C*) revealed a PPI equal to the TCL whilst entrainment on the posterior wall near the left pulmonary veins (*D*) showed a PPI-TCL of 92 ms. See also Supplementary material online, *Video S2*. *, left atrial appendage; LUPV, left upper pulmonary vein.

roof and contributing to difficulties in obtaining roof line block. Similar difficulties are encountered in ablation of the mitral isthmus with CS ablation required in over 50% in some studies.[17] We have shown an example of a roof-dependent LA flutter involving epicardial conduction across an ablated roof line (*Figure 3*), identified using non-contact mapping. A particular advantage of non-contact mapping is the rapid visualisation of whole chamber activation with less dependence on ensuring catheter contact with the whole atrial surface as required in collection of high-density contact maps. A largely automated processing technique then facilitates rapid visualization of tachycardia circuits allowing identification of the critical isthmus or focal origin. One disadvantage of this approach however is the inability to manually review and edit EGM points included within a map, which may result in map artefacts requiring caution in interpretation. In addition, analysis of charge density is in its infancy with work still required in how to deal with very low amplitude signals. This is particularly challenging when trying to assess block in ablated veins or isolation of the posterior wall, as was observed on one occasion in this study. Low amplitude far-field signals can often be detected within ablated veins using the high-resolution charge density approach making analysis of isolation particularly unreliable.

A higher number of virtual EGMs were used for non-contact charge density maps compared with contact mapping although neither this difference nor mapping time were statistically significant when maps of paced rhythms were analysed independently, partly due to the small sample size ($n = 6$). Assessing conduction through linear lesions can be achieved through collection of limited data that is adequate to demonstrate vectors of activation consistent with block or conduction through the ablated region. This can be achieved rapidly, and high-density catheters still collect multiple EGM points. Roving of the non-contact catheter requires collection of adequate data samples within each position to group beats accurately, with the lower atrial rate during pacing resulting in longer acquisition times. Non-contact catheter manipulation may also result in dislodging of additional catheters required for pacing (e.g. ablation catheter within the LAA), whilst additional manual processing of recorded data is required to generate paced maps, therefore reducing the time difference between the two mapping techniques.

It should be acknowledged that although mapping analysis was blinded and accuracy of each approach then compared to the final diagnosis made once the response to ablation is known, this method may not entirely exclude bias. A more robust comparison with clinical endpoints would require a prospective study with patients randomised to mapping technique. However, this was not the aim of this analysis, which was designed to evaluate the clinical utility of the SuperMap algorithm. It was not presumed that either technique would be superior in terms of diagnostic accuracy particularly given that, in clinical practice, results of electroanatomical mapping are routinely combined with additional clinical tools such as inspection of EGM morphology and entrainment manoeuvres.

Conclusion

In conclusion, SuperMap non-contact charge density mapping is a rapid and reliable approach to guide the ablation of complex ATs. Panoramic mapping may provide further opportunities to understand complex arrhythmia mechanisms, but further work is required to fully understand the analysis of charge density signals in assessing the atrial substrate.

Supplementary material

Supplementary material is available at *Europace* online.

Funding

This study was supported by the Oxford Biomedical Research Centre and funded by internal departmental budgets.

Conflict of interest: M.T.B.P. has received honoraria and support for conference attendance from Acutus Medical. T.R.B. has received honoraria from Acutus Medical and is a member of their Medical Advisory Board. All remaining authors have no conflicts to declare.

Data availability

Data are available from the corresponding author upon reasonable request.

References

1. Roberts-Thomson KC, Kistler PM, Kalman JM. Atrial tachycardia: mechanisms, diagnosis, and management. *Curr Probl Cardiol* 2005;**30**:529–73.
2. Kim YH, Chen SA, Ernst S, Guzman CE, Han S, Kalarus Z *et al.* 2019 APHRS expert consensus statement on three-dimensional mapping systems for tachycardia developed in collaboration with HRS, EHRA, and LAHRS. *J Arrhythm* 2020;**36**:215–70.
3. Rostock T, Drewitz I, Steven D, Hoffmann BA, Salukhe TV, Bock K *et al.* Characterization, mapping, and catheter ablation of recurrent atrial tachycardias after stepwise ablation of long-lasting persistent atrial fibrillation. *Circ Arrhythm Electrophysiol* 2010;**3**:160–9.
4. Grace A, Willems S, Meyer C, Verma A, Heck P, Zhu M *et al.* High-resolution noncontact charge-density mapping of endocardial activation. *JCI Insight* 2019;**4**:e126422.
5. Ramak R, Chierchia GB, Paparella G, Monaco C, Miraglia V, Cecchini F *et al.* Novel noncontact charge density map in the setting of post-atrial fibrillation atrial tachycardias: first experience with the Acutus SuperMap Algorithm. *J Interv Card Electrophysiol* 2021;**61**:197.
6. Shi R, Norman M, Chen Z, Wong T. Individualized ablation strategy guided by live simultaneous global mapping to treat persistent atrial fibrillation. *Future Cardiol* 2018;**14**:237–49.
7. Willems S, Verma A, Betts TR, Murray S, Neuzil P, Ince H *et al.* Targeting nonpulmonary vein sources in persistent atrial fibrillation identified by noncontact charge density mapping. *Circ Arrhythm Electrophysiol* 2019;**12**:e007233.
8. Chae S, Oral H, Good E, Dey S, Wimmer A, Crawford T *et al.* Atrial tachycardia after circumferential pulmonary vein ablation of atrial fibrillation: mechanistic insights, results of catheter ablation, and risk factors for recurrence. *J Am Coll Cardiol* 2007;**50**:1781–7.
9. Jais P, Shah DC, Haissaguerre M, Hocini M, Peng JT, Takahashi A *et al.* Mapping and ablation of left atrial flutters. *Circulation* 2000;**101**:2928–34.
10. Takigawa M, Derval N, Frontera A, Martin R, Yamashita S, Cheniti G *et al.* Revisiting anatomic macroreentrant tachycardia after atrial fibrillation ablation using ultrahigh-resolution mapping: implications for ablation. *Heart Rhythm* 2018;**15**:326–33.
11. Hung Y, Chang SL, Lin WS, Lin WY, Chen SA. Atrial tachycardias after atrial fibrillation ablation: how to manage? *Arrhythm Electrophysiol Rev* 2020;**9**:54–60.
12. Hayashi K, Mathew S, Heeger CH, Maurer T, Lemes C, Riedl J *et al.* Pace mapping for the identification of focal atrial tachycardia origin: a novel technique to map and ablate difficult-to-induce and nonsustained focal atrial tachycardia. *Circ Arrhythm Electrophysiol* 2016;**9**:e003930.
13. Wieczorek M, Salili AR, Kaubisch S, Hoeltgen R. Catheter ablation of nonsustained focal right atrial tachycardia guided by virtual non-contact electrograms. *Europace* 2011;**13**:876–82.
14. Winkle RA, Moskovitz R, Mead RH, Engel G, Kong MH, Fleming W *et al.* Ablation of atypical atrial flutters using ultra high density-activation sequence mapping. *J Interv Card Electrophysiol* 2017;**48**:177–84.
15. Takigawa M, Derval N, Martin CA, Vlachos K, Denis A, Nakatani Y *et al.* Mechanism of recurrence of atrial tachycardia: comparison between first versus redo procedures in a high-resolution mapping system. *Circ Arrhythm Electrophysiol* 2020;**13**:e007273.
16. Pambrun T, Duchateau J, Delgove A, Denis A, Constantin M, Ramirez FD *et al.* Epicardial course of the septopulmonary bundle: anatomical considerations and clinical implications for roof line completion. *Heart Rhythm* 2021;**18**:349–57.
17. Maheshwari A, Shirai Y, Hyman MC, Arkles JS, Santangeli P, Schaller RD *et al.* Septal versus lateral mitral isthmus ablation for treatment of mitral annular flutter. *JACC Clin Electrophysiol* 2019;**5**:1292–9.